To appear in ApJ

Detection of the 2175Å Extinction Feature at $z = 0.83$

V. Motta[1,2], E. Mediavilla[1], J. A. Muñoz[1], E. Falco[3], C.S. Kochanek[3], S. Arribas[4,5], B. García-Lorenzo [6], A. Oscoz[1], M. Serra-Ricart[1]

ABSTRACT

We determine the extinction curve in the $z_l = 0.83$ lens galaxy of the gravitational lens SBS0909+532 from the wavelength dependence of the flux ratio between the lensed quasar images ($z_s = 1.38$) from 3400 to 9200Å. It is the first measurement of an extinction curve at a cosmological distance of comparable quality to those obtained within the Galaxy. The extinction curve has a strong 2175Å feature, a noteworthy fact because it has been weak or non-existent in most estimates of extinction curves outside the Galaxy. The extinction curve is fitted well by a standard $R_V = 2.1 \pm 0.9$ Galactic extinction curve. If we assume standard Galactic extinction laws, the estimated dust redshift of $z = 0.88 \pm 0.02$ is in good agreement with the spectroscopic redshift of the lens galaxy. The widespread assumption that SMC extinction curves are more appropriate models for cosmological dust may be incorrect.

Subject headings: gravitational lensing, quasars: individual (SBS 0909+532), dust, extinction

[1]Instituto de Astrofísica de Canarias, Vía Láctea S/N, La Laguna 38200, Tenerife, Spain

[2]Departamento de Astronomía, Facultad de Ciencias, Iguá 4225, Montevideo 11400, Uruguay

[3]Harvard-Smithsonian Center for Astrophysics, 60 Garden Street, Cambridge, MA 02138, USA

[4]Space Telescope Science Institute. 3700 San Martin Drive, Baltimore, MD21218, USA. Affiliated with the Research and Science Support Department of ESA. On leave from the Instituto de Astrofísica de Canarias

[5]Consejo Superior de Investigaciones Científicas

[6]Isaac Newton Group of Telescopes, 38700 S/C de La Palma, Spain

1. INTRODUCTION

Just as the properties of galaxies and stars evolve with cosmic time, so must the properties of the interstellar medium. In particular, with changes in metallicity and ionizing backgrounds we might expect the properties of dust to change with redshift. Locally we can make precise measurements of extinction curves as a probe of the dust grains by comparing the spectral energy distributions (SED) of reddened and unreddened stars of the same spectral type (the pair method, Massa, Savage & Fitzpatrick (1983)), but the need to measure the spectra of individual stars limits this approach to the Galaxy, its satellites and its nearest neighbors.

The average Galactic extinction curve is well modeled over a broad wavelength range as a function of only the ratio of total to selective extinction, R_V (e.g. Cardelli, Clayton & Mathis 1989, hereafter CCM; Fitzpatrick 1999). These extinction curves include a spectral feature, the 2175Å bump, and appear to apply to a wide range of interstellar dust environments in the Galaxy. It is not, however, a universally valid law. While some lines of sight in the Magellanic clouds show similar extinction laws, others, like the 30 Doradus region of the Large Magellanic Cloud (LMC) show weaker 2175Å features and steeper far UV extinction curves (e.g., Fitzpatrick 1986). The most extreme deviations from the Galactic extinction curves are found in the bar of the Small Magellanic Cloud (SMC, Gordon & Clayton 1998). Some newer studies (e.g., Clayton, Gordon & Wolff 2000) have found lines of sight with weak 2175Å features and steep far UV extinctions in the Galaxy as well. M31 is the most distant galaxy to which the pair method can be applied; the M31 extinction curve seems similar to that of the Galaxy but may have a weaker 2175Å bump (Bianchi et al. 1996).

The studies of extinction in other galaxies are in many cases based on the examination of the attenuation induced by dust in the SED of the galaxies. But the physical properties of dust and its geometrical distribution affect in a complex way the intrinsic SED of the galaxy stellar population, which must be also modeled. The extinction curves inferred from these indirect methods are strongly model-dependent and, in many cases, not unique due to model degeneracies (Bianchi et al. 1996; Gordon, Calzetti & Witt 1997). In M33, Gordon et al. (1999) noticed that a depression found in the SED should be related to the 2175Å feature, according to a radiative transfer model including attenuation by dust. A very weak 2175Å feature is also found by Rosa & Benvenuti (1994) by comparing spectra of ionizing star clusters in HII regions of M101 with population synthesis models. However, the modeling of the SED of 30 starburst galaxies (Gordon, Calzetti & Witt 1997) implies that the dust has extinction properties similar to that of the SMC, lacking a 2175Å feature.

Some efforts have also been made in AGNs to study the effects of extinction by comparing the observed SEDs with conveniently selected templates. Crenshaw et al. (2001) have

compared the spectra of the Seyfert 1 galaxies NGC 3227 and NGC 4151 (assumed unreddened), and found that the extinction in NGC 3227 increases very steeply toward the far UV (steeper than in the SMC) and that there is no evidence of the 2175Å bump. In QSOs, the comparison of the observed spectra with composite spectra has not revealed traces of the 2175Å feature (Pitman & Clayton 2000; Vanden Berk 2001). All the above-mentioned studies suggest that the presence of a significant 2175Å bump in the average extinction curve of the Milky Way is rare (Pitman & Clayton 2000). In any case, the validity of this or any other conclusion about the behavior of the extinction beyond the Local Group is limited by the lack of a direct method to obtain the extinction curve. This limitation has serious consequences for the study of galaxies (see Gordon et al. 2000, and references therein) and in cosmology (see Falco, Kochanek & Muñoz 1998, and references therein).

There are now two techniques which can extend the measurement of precise extinction curves into the realm of cosmology. One is based on the use of the relationship between the variations in color and absolute magnitude in SNIa light curves (Riess, Press & Kirshner 1996). This technique has been used to estimate several reddening ratios from nearby supernovae which are in agreement with the MW average extinction curve. The other is an extension of the standard pair method to obtain extinction curves in gravitational lens galaxies. The method compares two different images of the same lensed QSO which follow different paths through the lens galaxy (Nadeau et al. 1991). As in the pair method each image has the same intrinsic spectrum but suffers from a different amount of extinction along each path through the lens galaxy. Using broad-band optical and NIR photometry, Falco et al. (1999) measured differential extinctions in 23 gravitational lens galaxies. In spite of the coarse spectral sampling, Falco et al. (1999) could fit the average Galactic extinction law to several lens galaxies, finding values for R_V in the range 0.64 to 7.2. This range includes some extreme values for R_V whose physical significance is not obvious as the CCM law was inferred from values of R_V in the 2.5 to 5.5 range. Falco et al. (1999) also derived relatively accurate dust redshifts following the technique proposed by Jean & Surdej (1998). These studies relied on broad band photometry, which can lead to problems distinguishing between extinction and gravitational microlensing and cannot provide complete extinction curves over broad wavelength ranges. These problems can be overcome using spectra of the individual images, particularly using integral field spectroscopy (IFS) to obtain a 2D array of spectra of the lens and its images (Mediavilla et al. 1998).

In this article, we use IFS to search for the 2175Å feature in a cosmologically distant galaxy by selecting a gravitational lens where the lens galaxy shows significant extinction and the redshifted wavelength of the 2175Å feature, $2175(1+z_l)$Å is below the Lyman break in the spectrum of the source quasar at $912(1+z_s)$Å. We performed the experiment on the two-image, $1\farcs11$ separation quasar lens SBS 0909+532 (Kochanek et al. 1997), where the

$z_l = 0.83$ lens and $z_s = 1.38$ source redshifts (Oscoz et al. 1997; Lubin et al. 2000) satisfy the wavelength criterion, and Falco et al. (1999) found there was significant differential extinction $\Delta E(B-V) = 0.20 \pm 0.03$ based on the image flux ratios measured in broad band imaging.

2. DATA ANALYSIS

2.1. Observations and Data Reduction

The spectra of SBS 0909+532 were taken on January 18, 2001 with the 2D-fiber system INTEGRAL (Arribas et al. 1998), at the 4.2-m William Herschel Telescope (WHT). INTEGRAL links the Nasmyth focus of the WHT with the WYFFOS spectrograph. We used the SB1 fiber bundle that consists of a rectangular array of 175 fibers, each $0\farcs45$ in diameter, covering an area of $7\farcs9 \times 6\farcs7$ on the sky, and a ring with diameter $90''$ formed by 30 fibers of the same size as those in the inner array. The distance between adjacent fibers is $0\farcs5$ in the central rectangle. At the entrance of the spectrograph, the fibers are aligned to form a pseudo-slit.

We took three exposures of 1800s each. We used the 300lines/mm grating, R300B, that yields a linear dispersion of 6.0Å pixel^{-1} covering the wavelength range from 3400 to 9200Å. The seeing, measured from a guide star was $\sim 1''$.

For our data reduction, we used the `IRAF`[7] software package. The procedure included bias subtraction, cosmic-ray rejection, spectra extraction, throughput correction, wavelength calibration, and sky subtraction. All these steps were applied to each one of the three individual frames and to an average frame obtained by combining them. For additional details on reduction and analysis of data taken with optical fibers, see Arribas, Mediavilla & Rasilla (1991).

In Figure 1 we show the 2D distribution of spectra from the average frame over a spectral range from 6000 to 7200 Å including the MgIIλ2798 emission line. The positions of the two compact components A and B are also shown.

[7] `IRAF` is distributed by the National Optical Astronomy Observatories, which is operated by the Association of Universities for Research in Astronomy, Inc. (AURA) under cooperative agreement with the National Science Foundation

2.2. Continuum Maps

From the 2D collection of spectra corresponding to the averaged frame (a subset of them around components A and B is shown in Figure 1) we interpolated 20 continuum maps covering all the observed spectral range. The central wavelengths and widths of the continua are included in Table 1. We fitted and removed the strong emission lines present in the QSO spectra.

In Figure 2 we present six of these continuum maps corresponding to the averaged frame centered at 8727Å, 7233Å, 5739Å, 4447Å, 4006Å, and 3487Å. The two compact components of SBS 0909+532 appear well separated in the reddest map (8727Å, seeing$\sim 1\farcs05$). Notice the continuous fading of image B from the red to the blue maps. In fact, in the bluest map (3487Å) the B image is no longer visible. This decrease in the B/A flux ratio towards the blue is explained by dust absorption in the lensing galaxy (Falco et al. 1999).

2.3. A and B Spectra

Because of differential atmospheric refraction (DAR), the location of any of the components in the telescope focal plane changes with wavelength. In fact, we measured a displacement of about $0\farcs6$ (greater than the diameter of a fiber face) between the bluest and reddest continuum maps. Although the displacement is modest, it implies that none of the spectra of Figure 1 can be exactly identified with one of the components throughout the full spectral range. This is a general problem of spectroscopy in a large spectral range that admits an *a posteriori* correction when 2D spectroscopy is available (Arribas et al. 1999). Following the procedure described in this reference, we calculated a DAR model from the location of component A in the 20 continuum maps distributed along the full spectral range. Next, from the original spectra we interpolated a new 2D set of spectra corrected for DAR (see Arribas et al. 1999 for the details). From these spectra we obtained a map in the 3500-9000Å spectral range. We located the centroid of the A component in this map and used the coordinates offset of B from A given in Lehár et al. (2000) to infer the location of the B component. Finally, we interpolated at these locations the A and B spectra (see Figure 3) from the ensemble of spectra corrected for DAR. The changes from the uncorrected spectra are modest, as expected.

3. RESULTS

3.1. Differential Extinction Curve from Continuum Images

To derive the B/A flux ratios from the ensemble of continuum maps covering the full observed spectral range, we fit the maps using PSFs derived from the continuum images of a star observed on the same night. We used as fitting parameters the separation between the two QSO images, their relative intensity, the sky background, and the blurring of the PSF due to the seeing. We followed this procedure with each one the three independent exposures. After subtracting the quasar model, the pattern of residuals show no emission from the galaxy at any wavelength, so we conclude that our photometric model with only two point-like sources reproduces successfully the observed continua. Acording to the HST data (Lehár et al. 2000) the lens galaxy is not detected in the V band and its integrated magnitude is only 5% of component A flux in the I band. The location of the two quasar components determined by our photometric model is in excellent agreement with the results obtained with the HST by Lehár et al. (2000) which strengthens the validity of our photometric decomposition.

In Table 1 and Figure 4 we present the mean magnitude differences, $m_B - m_A$, derived from the PSF fitting. To estimate the errors we have used the dispersion between the results obtained from each independent exposure. We include in this Figure the $m_B - m_A$ differences from Lehár et al. (2000) and Kochanek et al. (1997) corresponding to broad band data; the agreement is excellent.

3.2. Differential Extinction Curve from Emission Line Images

Proceeding in the same way as for the continua, we have also computed the $m_B - m_A$ differences for the emission in the MgIIλ2798 and CIII]λ1909 lines. To estimate and subtract the continuum below each line, we fitted a straight line to adjacent points. The magnitude differences in the emission lines are approximately 0.3 mag above that of the continuum ($m_B - m_A$, see Figure 4). These differences are probably created by microlensing from the stars in the lens galaxy which can differentially magnify the continuum and emission line regions of the quasar because of their differing physical sizes (Schneider, Ehlers & Falco 1988). While there are too few emission lines to estimate an extinction curve, the emission lines are consistent with the extinction properties estimated from the continuum. We have also tried to compute the $m_B - m_A$ difference from the CIV]λ1548, but the maps were too noisy and the results of the PSF fitting were not consistent.

Table 1.

λ[a]	W[b]	m_B-m_A[c]	$\Delta(m_B$-$m_A)$[d]
3487	252	1.40	0.20
3565	96	1.45	0.06
3661	96	1.59	0.05
3757	96	1.67	0.12
3853	96	1.83	0.10
3949	96	1.77	0.13
4063	96	1.75	0.10
4159	96	1.63	0.17
4255	96	1.52	0.08
4351	96	1.52	0.08
4447	96	1.35	0.09
4743	498	1.07	0.08
5241	498	0.91	0.03
5739	498	0.83	0.02
6237	498	0.69	0.02
6735	498	0.55	0.03
7233	498	0.47	0.03
7731	498	0.43	0.03
8229	498	0.37	0.02
8727	498	0.37	0.02

[a]Central wavelength of the continuum maps (Å)

[b]Wavelength bin of the continuum maps (Å)

[c]Average magnitude differences

[d]Error in magnitude differences

3.3. Differential Extinction Curve from A and B Uncontaminated Spectra

The method followed in Section 3.1 could be repeated with narrower continua to obtain the differential extinction curve with improved spectral sampling that could even match the spectral resolution of the data. However, the spectral sampling that can be achieved with this method is, in practice, limited by the noise in the data and the PSF.

To improve the spectral resolution we can try, alternatively, and only because the lens galaxy is undetected, to obtain the extinction curve directly from the A and B spectra after correcting them for the cross-contamination induced by the seeing. We can estimate the contribution of A to the spectrum measured at the position of B by measuring the spectrum at position C located at the same distance from A as in the image B but in the opposite direction (see Figure 1). Similarly we obtain spectrum D as an estimate of the contribution to A from B. Our estimate of the seeing-corrected spectra are the differences $A_u = A - D$ and $B_u = B - C$.

We can check the results by comparing the spectral ratio to the estimates made by directly fitting the continuum maps. They agree reasonably well, with a ~ 0.15 mag drift between the blue and the red wavelengths. The drift appears to be due to small asymmetries in the PSF. We can improve the agreement by defining $A_u = A - (1-\epsilon)D$ and $B_u = B-(1+\epsilon)C$ with $\epsilon = 0.1$ to correct for the asymmetries. Figure 5 shows our final estimate of the magnitude differences $[m_{B_u} - m_{A_u}](1/\lambda_0)$ after smoothing by a $\sigma = 30$Å Gaussian. This curve is in good agreement with the difference magnitudes obtained from the continuum images at all wavelengths except in the vicinity of the emission lines. As stated in the previous section, this could arise from microlensing that is not affecting the lines to the same degree as the continuum. This implies that, in some spectral regions (like the one including the CIVλ1548 line in SBS 0909+532) observations made with narrow-band filters could be problematic for obtaining the extinction curves since the contribution from the continuum and the strong emission lines must be separated. (Notice also the presence of the Mg II$\lambda\lambda$2796,2803 absorption doublet arising from the lens galaxy).

4. DISCUSSION

Assuming that any microlensing effects are achromatic, the magnitude difference (Figure 4) is a simple function of the magnification ratio ΔM in magnitudes, the differential extinction $\Delta E(B-V)$ and the extinction law $R(\lambda)$ (Falco et al. 1999),

$$m_B(\lambda) - m_A(\lambda) = \Delta M + \Delta E(B-V)\, R\left(\frac{\lambda}{1+z_l}\right). \qquad (1)$$

We fitted the $m_A - m_B$ data from the continua using equation (1) and the CCM parameterization of the extinction curve $R(\lambda)$. In a first step, the redshift is restricted to the value determined directly from the absorption lines of the lens galaxy ($z = 0.83$). The best fit is obtained for $R_V = 2.1 \pm 0.9$, $\Delta M = -0.2 \pm 0.2$ and differential extinction $\Delta E(B-V) = 0.21 \pm 0.02$. A visual inspection of the fit (see Figure 4) shows reasonable agreement with the CCM extinction curve for the MW ($\chi^2/dof \sim 2$). In spite of the uncertainties in R_V, the fit of the 2175Å bump is good in both shape and central wavelength. When, in a second step, changes not only in R_V but also in z were allowed, we found that R_V was very poorly determined, but we obtained a useful estimate for the redshift, $z = 0.88 \pm 0.02$. The close agreement with the spectroscopic redshift of the lens galaxy ($z = 0.83$, Oscoz et al. 1997; Lubin et al. 2000) demonstrates the possibilities of the dust-redshift technique (Jean & Surdej 1998; Falco et al. 1999) and reinforces the reliability of the extinction law.

The detection of a significant 2175Å feature in the extinction curve of a galaxy at $z = 0.83$ is very noteworthy. Many extragalactic extinction studies have suggested that the 2175Å feature is rare (see Pitman & Clayton 2000, and references therein). However, these studies were based mainly on starburst galaxies and AGNs, where the dust is subject to processing by radiation and shocks, similar to the environments of star formation regions of the LMC or the SMC, where the 2175Å bump is weak. Thus, the detection of this feature in the extinction curve of the SBS 0909+532 lens (a normal early-type galaxy) and its absence in active galaxies follows naturally under the hypothesis of a connection between activity and suppression of the 2175Å feature.

It has been proposed that the presence of the 2175Å feature is anti-correlated with the FUV extinction, with the feature weakening as the FUV extinction steepens (Clayton, Gordon & Wolff 2000). Accordingly, the rather low value $R_V = 2.1$ (although not rare in the extragalactic domain, see Falco et al. 1999 and references therein) that implies a steep FUV rise would be inconsistent with the strong bump (e.g. HD 210121, Clayton, Gordon & Wolff 2000). Within the uncertainty of the determination of R_V the average value for the MW ($R_V = 3.1$) would also be acceptable and in better accordance with the presence of a significant bump. Additional UV and IR data would be needed to better answer this question.

5. CONCLUSIONS

The application of the standard pair method to spectroscopic observations of the gravitationally lensed QSO SBS 0909+532 has allowed us to obtain the first determination of an

UV extinction law beyond the Local Group. Our conclusions are:

1. We have detected a significant 2175Å bump in a $z = 0.83$ galaxy. So far, most studies of extinction in the extragalactic domain have been based on starburst and AGN galaxies which seem to exhibit SMC-like dust properties lacking a 2175Å feature. However, the lens galaxy of SBS 0909+532 seems to contain dust like that of the Galaxy.

2. The Cardelli, Clayton & Mathis (1989) law provides a reasonable fit to the SBS 0909+532 extinction curve with $R_V = 2.1 \pm 0.9$. This value includes, at $\sim 1\sigma$, the average MW law ($R_V = 3.1$). However, values of $R_V \lesssim 2.1$ will be difficult to reconcile with the proposed experimental correlation between weak bumps and steep FUV extinction.

3. The lens redshift estimated from the dust, $z_{dust} = 0.88 \pm 0.02$, agrees well with the redshift inferred from the absorption lines of the lens galaxy.

We know of about 70 gravitational lenses, many of which show signs of differential extinction (Falco et al. 1999). By applying our techniques to a wider sample of these lenses we should be able to provide a broad outline of the properties and potentially the evolution of extinction curves with cosmic time.

The WHT is operated on La Palma by the Isaac Newton Group (ING) of Telescopes in the Spanish Observatory Roque de los Muchachos of the Instituto de Astrofísica de Canarias (IAC). We would like to thank the support astronomer A. García Pérez and the night assistant N. Mahoney. This work was supported by the P6/88 project of the IAC. V. Motta acknowledges the support of a MUTIS Fellowship from the Agencia Española de Cooperación Internacional (AECI). E.E. Falco & C.S. Kochanek were partially supported by NASA through the grant GO-8252 from the Space Telescope Science Institute, which is operated by the Association of Universities for Research in Astronomy, Inc.

REFERENCES

Arribas, S. et al. 1998, SPIE, 3355, 821

Arribas, S., Mediavilla, E., García-Lorenzo, B., del Burgo, C., and Fuensalida, J.J. 1999, A&AS, 136, 189

Arribas, S., Mediavilla, E., Rasilla, J.L. 1991, ApJ, 369, 260

Bianchi, L., Clayton, G.C., Bohlin, R.C., Hutchings, J.B., and Massey, P. 1996, ApJ, 471, 203

Cardelli, J.A., Clayton, G.C., and Mathis, J.S. 1989, ApJ, 345, 245

Clayton, G.C., Gordon, K.D., and Wolff, M.J. 2000, ApJS, 129, 147

Crenshaw, D.M., Kraemer, S.B., Bruhweiler, F.C., and Ruiz, J.R. 2001, ApJ, 555, 633

Falco, E. E., Impey, C. D., Kochanek, C. S., Lehár, J., McLeod, B. A., Rix, H.-W., Keeton, C. R., Muñoz, J. A., and Peng, C. Y. 1999, ApJ, 523, 617

Falco, E. E., Kochanek, C. S., and Muñoz, J. A 1998, ApJ, 494, 47

Fitzpatrick, E.L. 1986, AJ, 92, 1068

Fitzpatrick, E.L. 1999, PASP, 111, 63

Gordon, K.D., Calzetti, D., and Witt, A.N. 1997, ApJ, 487, 625

Gordon, K.D., and Clayton, G.C. 1998, ApJ, 500, 816

Gordon, K.D., Hanson, M.M., Clayton, G.C., Rieke, G.H., and Misselt, K.A. 1999, ApJ, 519, 165

Gordon, K.D., Clayton, G.C., Witt, A.N., and Misselt, K.A. 2000, ApJ, 533, 236

Jean, C., and Surdej, J. 1998, A&A, 339, 729

Kochanek, C.S., Falco, E.E., Schild, R., Dobrzycki, A., Engels, D., and Hagen, H.J. 1997, ApJ, 479, 678

Lehár, J., , Falco, E. E., Kochanek, C. S., McLeod, B. A., Muñoz, J. A., Impey, C. D., Rix, H. W., Keeton, C. R., and Peng, C. Y. 2000, ApJ, 536, 584

Lubin, L. M., Fassnacht, C. D., Readhead, A. C. S., Blandford, R. D., and Kundic, T. 2000, ApJ, 119, 451

Mediavilla, E. et al. 1998, ApJ, 503, L27

Massa, D., Savage, B.D., and Fitzpatrick, E.L. 1983, ApJ, 266, 662

Nadeau, D., Yee, H. K. C., Forrest, W. J., Garnett, J. D., Ninkov, Z., and Pipher, J. L. 1991, ApJ, 376, 430

Oscoz, A., Serra-Ricart, M., Mediavilla, E., and Buitrago, J. 1997, ApJ, 491, L7

Pitman, K.M., and Clayton, G.C. 2000, PASP, 112, 537

Riess, A. G., Press, W.H., and Kirshner, R.P. 1996, ApJ, 473, 588

Rosa, M.R., and Benvenuti, P. 1994, A&A, 291, 1

Schneider, P., Ehlers, J. and Falco, E.E. 1988, Gravitational lensing, Springer-Verlag: Berlin

Vanden Berk, D.E. et al. 1995, SPIE, 2476, 46

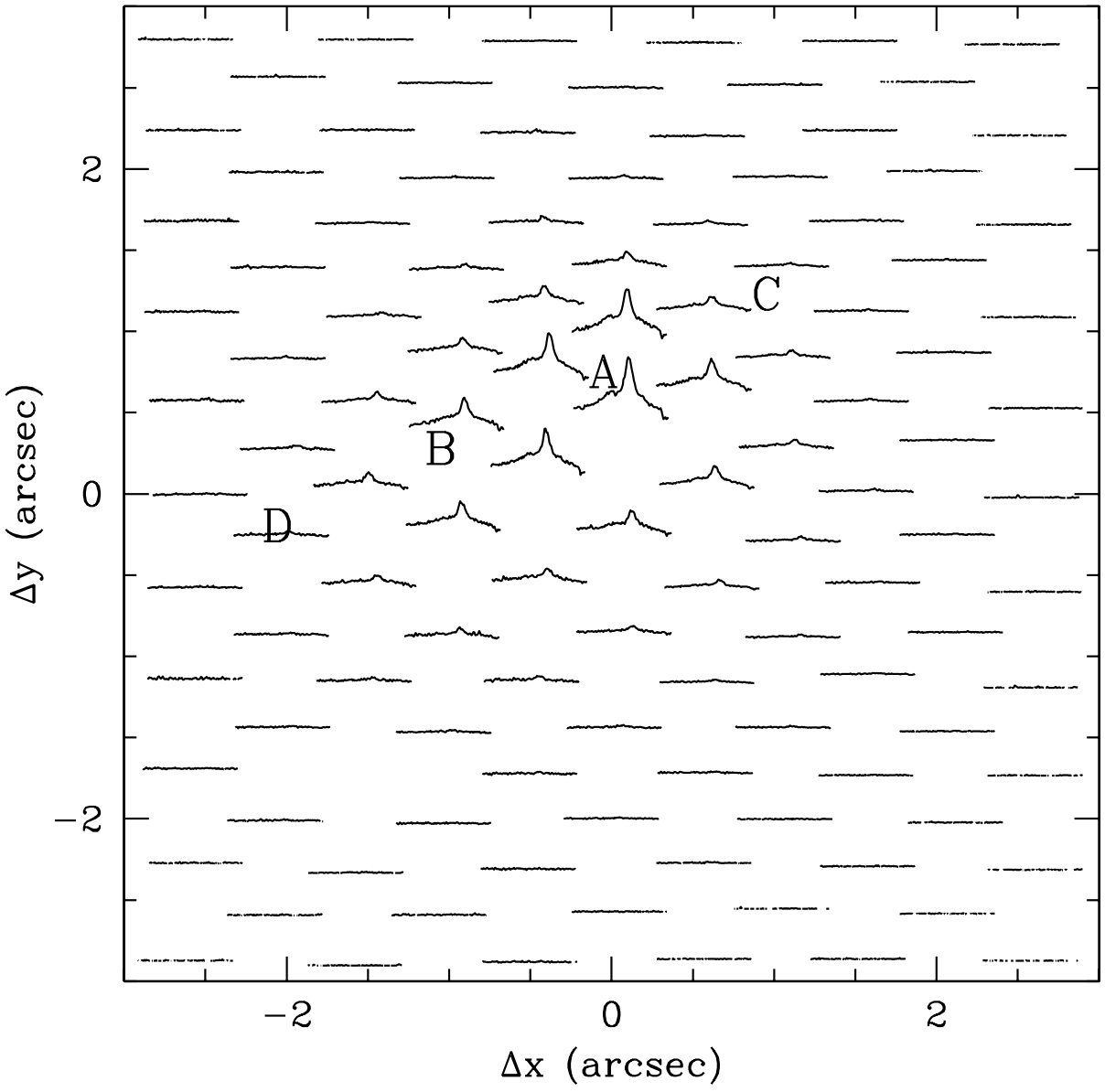

Fig. 1.— The 2D distribution of spectra around the A and B components, in the 6000 - 7200Å wavelength range. The locations of the two QSO images are marked A and B. C and D mark the locations where two spectra were interpolated to correct the effects of seeing in the A and B spectra (see section 3.3)

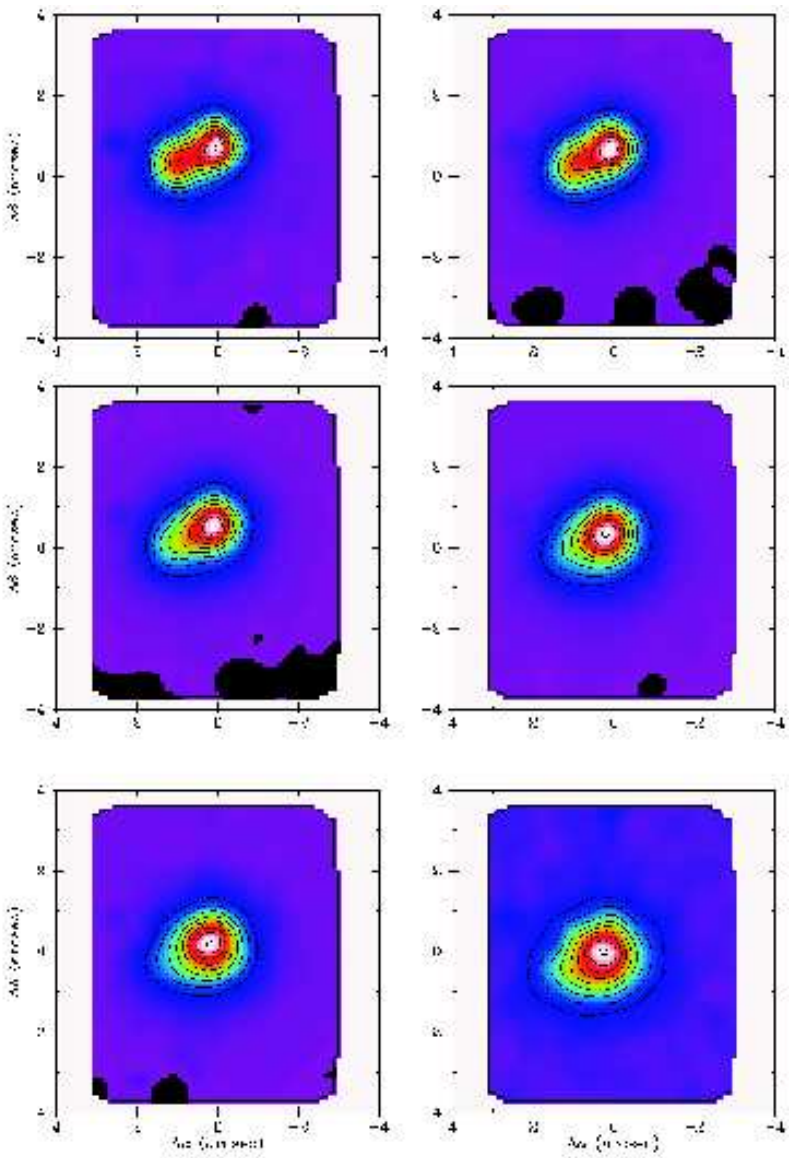

Fig. 2.— The plots shows 6 of the 20 continuum maps described in the text. From top to bottom, left to right, the continuum central wavelengths are 8727Å, 7233Å, 5739Å, 4447Å, 4006Å, and 3487Å.

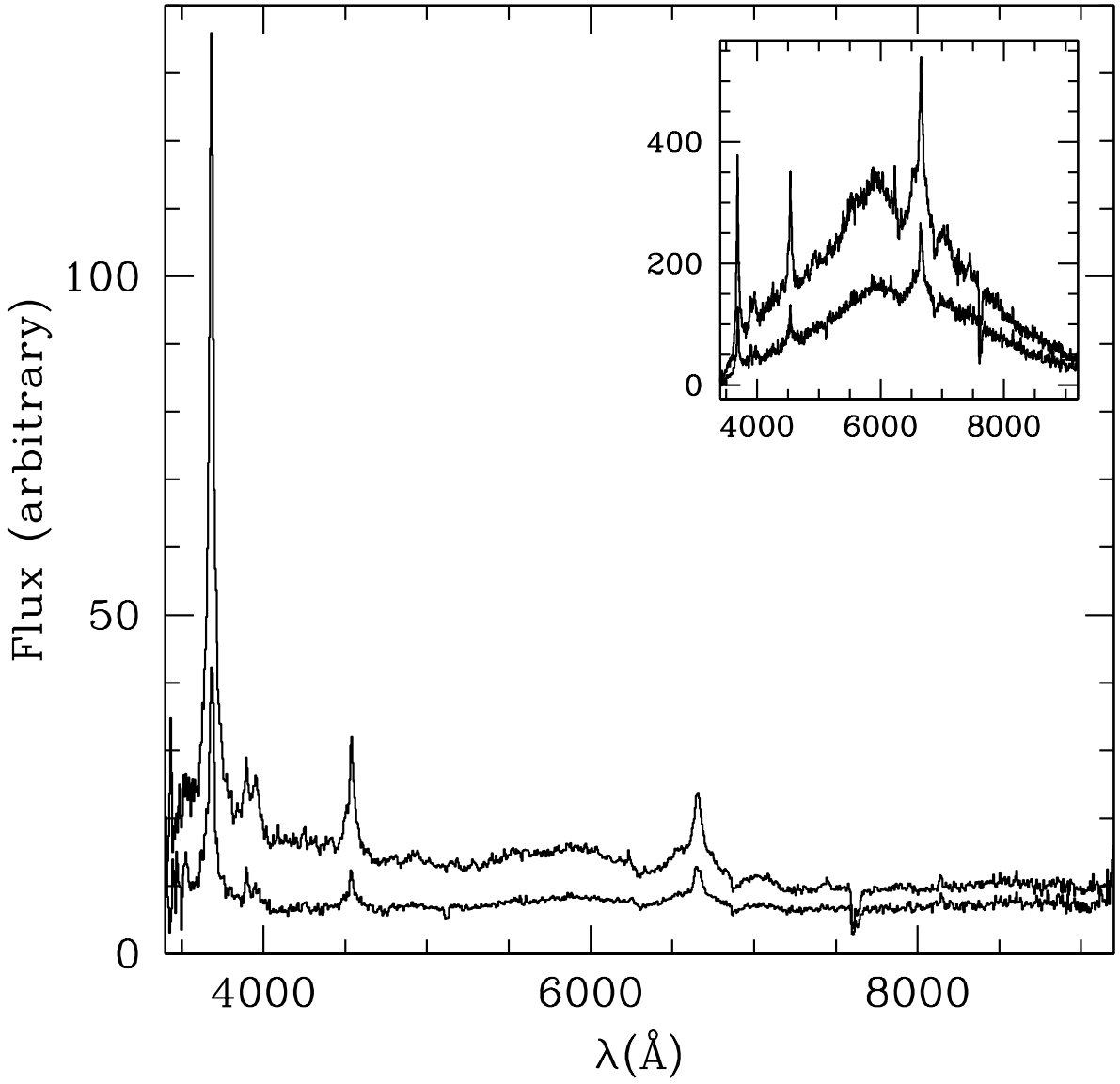

Fig. 3.— Spectra corresponding to the A and B QSO images corrected for the detector response. The small box shows the original spectra.

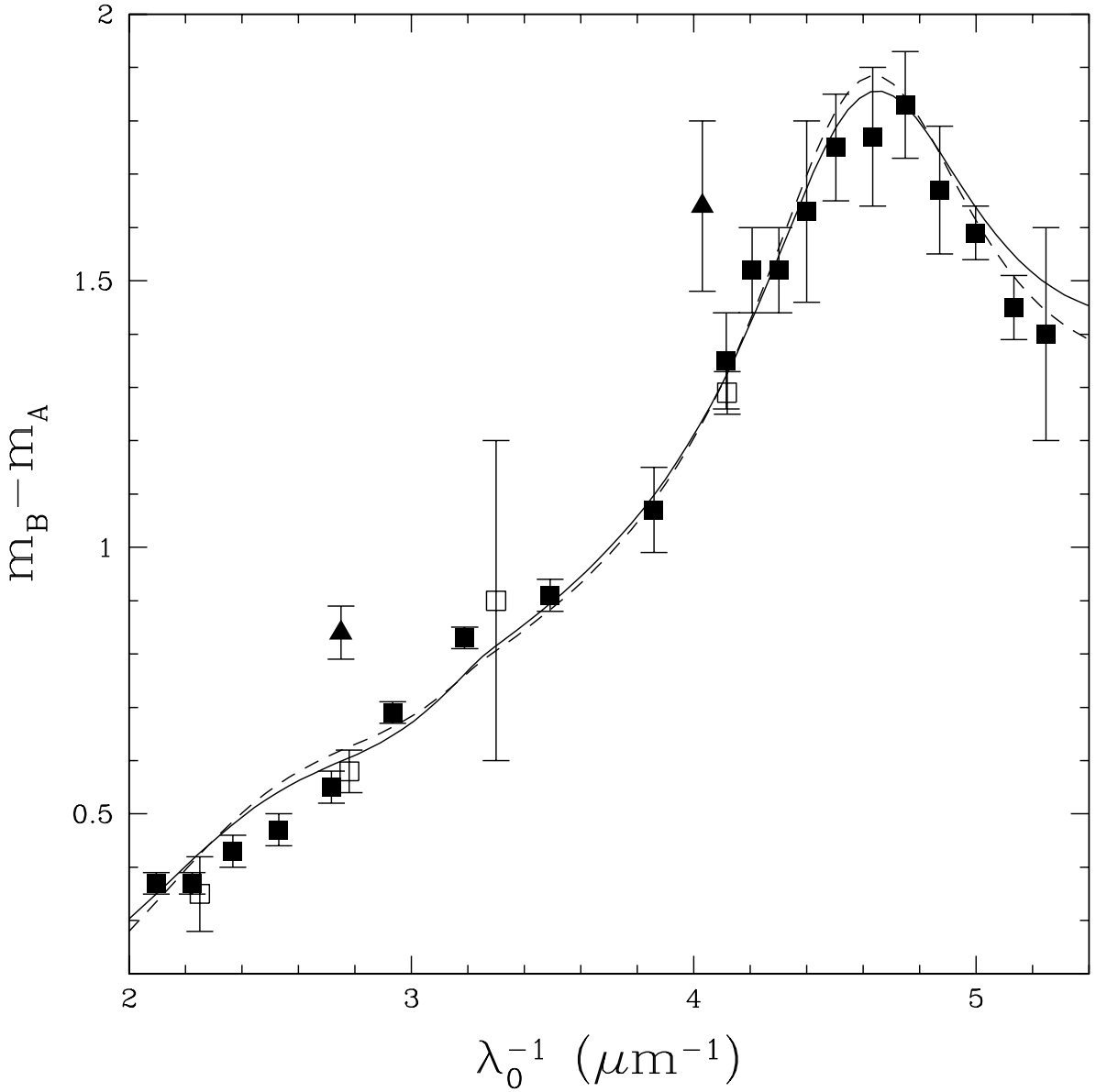

Fig. 4.— Magnitude differences $m_B - m_A$ obtained from continuum images as a function of inverse wavelength in the lens galaxy rest frame (filled squares). Open squares correspond to the B, V, R, I broad-band observations (Kochanek et al. 1997; Lehár et al. 2000). The solid line is the best fit of the analytical average MW extinction law to the observed extinction curve (filled squares) for a fixed $z = 0.83$. The values $R_V = 2.1 \pm 0.9$ and differential extinction $E(B-V) = 0.21 \pm 0.02$ were obtained in the fit. The filled triangles correspond to the $m_B - m_A$ differences computed from the emission in the MgII and CIII] lines. The dashed line corresponds to the best fit for $R_V = 3.1$.

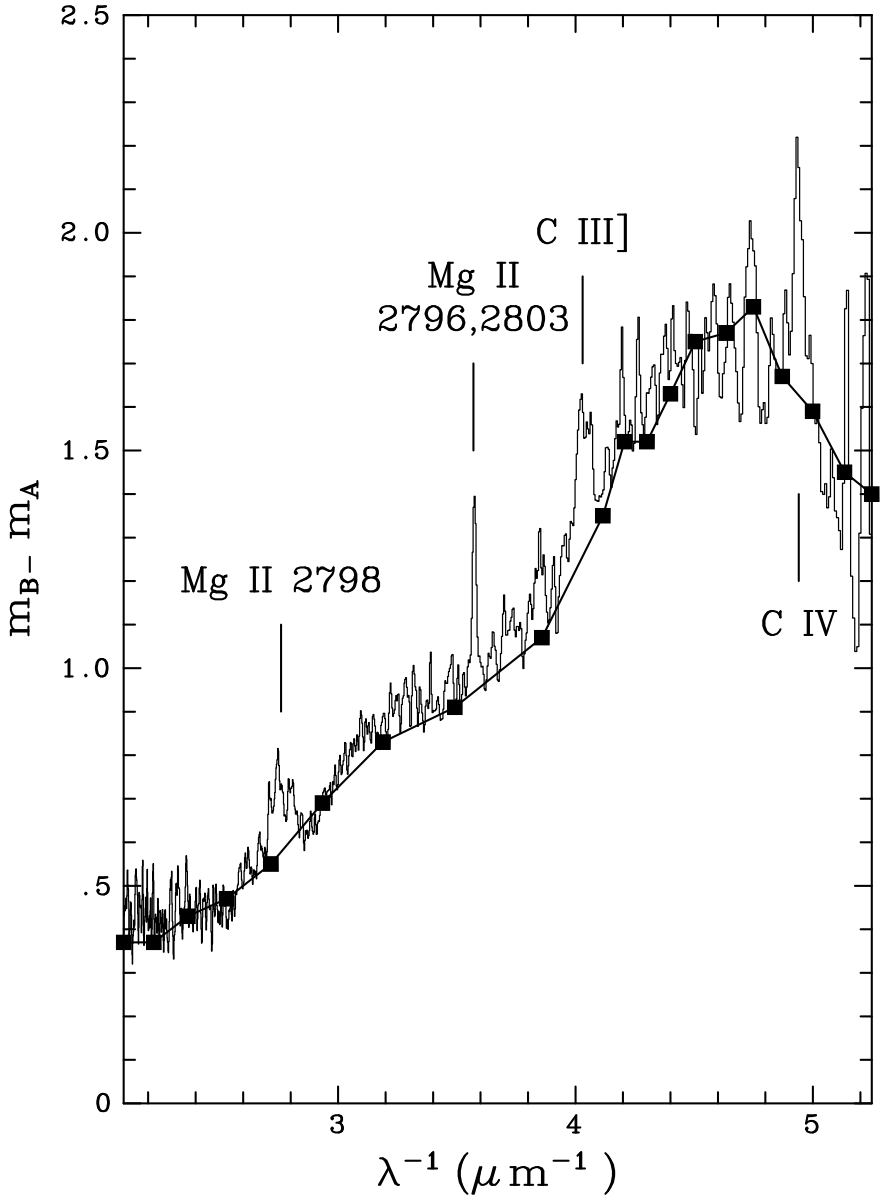

Fig. 5.— The continuous line is the $m_{B_u} - m_{A_u}$ magnitude difference curve obtained from the A and B spectra. The abscissa is the inverse wavelength at the lens galaxy rest frame. The squares joined by straight lines correspond to the data presented in Figure 4.